iScience

CellPress
OPEN ACCESS

Article

Tetraspanin CD53 Promotes Lymphocyte Recirculation by Stabilizing L-Selectin Surface Expression

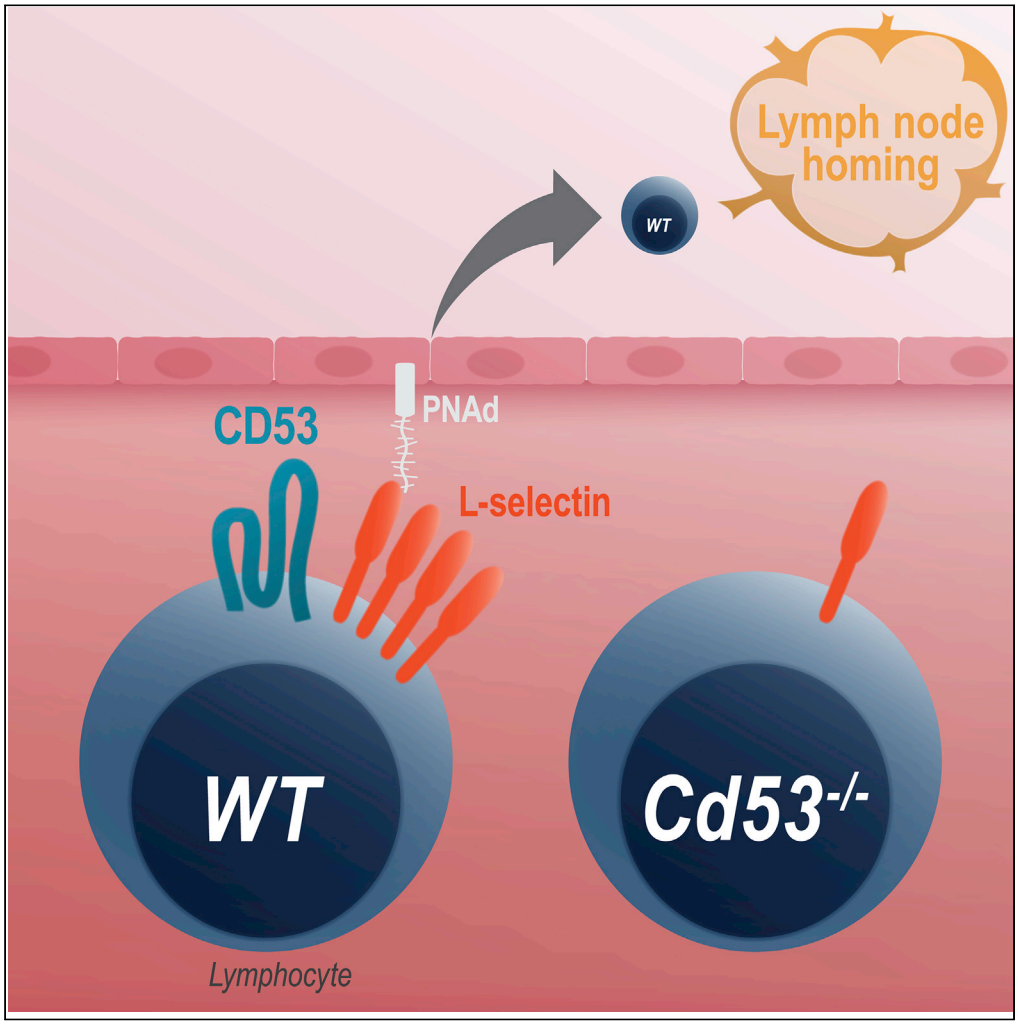

Maria C. Demaria, Louisa Yeung, Rens Peeters, ..., Annemiek van Spriel, Michael J. Hickey, Mark D. Wright

mark.wright@monash.edu

HIGHLIGHTS

CD53 is essential for lymph node cellularity as *Cd53*$^{-/-}$ lymph nodes lack T and B cells

CD53 is essential for lymphocyte homing to lymph nodes

CD53 stabilizes L-selectin cell surface expression and may restrain shedding

Impaired lymphocyte homing leads to diminished immune responses in *Cd53*$^{-/-}$ mice

Demaria et al., iScience *23*, 101104
May 22, 2020
https://doi.org/10.1016/j.isci.2020.101104

iScience

CellPress
OPEN ACCESS

Article

Tetraspanin CD53 Promotes Lymphocyte Recirculation by Stabilizing L-Selectin Surface Expression

Maria C. Demaria,[1] Louisa Yeung,[1,2] Rens Peeters,[3] Janet L. Wee,[1,2] Masa Mihaljcic,[1] Eleanor L. Jones,[1] Zeyad Nasa,[1] Frank Alderuccio,[1] Pamela Hall,[2] Brodie C. Smith,[2] Katrina J. Binger,[4] Gunther Hammerling,[5] Hang Fai Kwok,[6] Andrew Newman,[7] Ann Ager,[7] Annemiek van Spriel,[3] Michael J. Hickey,[2] and Mark D. Wright[1,8,*]

SUMMARY

Tetraspanins regulate key processes in immune cells; however, the function of the leukocyte-restricted tetraspanin CD53 is unknown. Here we show that CD53 is essential for lymphocyte recirculation. Lymph nodes of *Cd53*$^{-/-}$ mice were smaller than those of wild-type mice due to a marked reduction in B cells and a 50% decrease in T cells. This reduced cellularity reflected an inability of *Cd53*$^{-/-}$ B and T cells to efficiently home to lymph nodes, due to the near absence of L-selectin from *Cd53*$^{-/-}$ B cells and reduced stability of L-selectin on *Cd53*$^{-/-}$ T cells. Further analyses, including on human lymphocytes, showed that CD53 stabilizes L-selectin surface expression and may restrain L-selectin shedding via both ADAM17-dependent and ADAM17-independent mechanisms. The disruption in lymphocyte recirculation in *Cd53*$^{-/-}$ mice led to impaired immune responses dependent on antigen delivery to lymph nodes. Together these findings demonstrate an essential role for CD53 in lymphocyte trafficking and immunity.

INTRODUCTION

To initiate an adaptive immune response, antigen selects and clonally expands rare antigen-specific lymphocytes from a vast repertoire of specificities. The frequency of antigen-specific lymphocytes within the naive repertoire is minute, estimated in mice to be as low as 15–20 cells per animal (Moon et al., 2007; Obar et al., 2008), whereas in humans, frequencies can range from 0.6 to 6 cells per million cells (Alanio et al., 2010; Chu et al., 2009). It is therefore not surprising that the immune system has evolved strategies to maximize the chances of a successful encounter between antigen and rare antigen-specific lymphocytes. To this end, naive lymphocytes constantly patrol throughout the body, recirculating through the peripheral lymph nodes via interactions within specialized high endothelial venules (HEVs). Then, upon dwelling in the lymph nodes for 12–24 h, they return to the vasculature via the efferent lymphatics, enabling them to visit further peripheral lymph nodes (Gowans, 1959; Smith and Ford, 1983; Springer, 1994).

Many of the molecular interactions that govern the egress of naive lymphocytes at HEVs are well understood, and the key molecule responsible for lymph node homing is the membrane receptor L-selectin (Grailer et al., 2009; Springer, 1994). L-selectin mediates carbohydrate-based interactions with its HEV-expressed ligands termed peripheral node addressin, thus initiating the tethering and rolling of naive lymphocytes within HEVs (Streeter et al., 1988) and ultimately leading to stable adhesion and transmigration of naive lymphocytes into the lymph nodes (Ivetic, 2013). Essential to the control of lymphocyte trafficking is the tight regulation of L-selectin expression. Upon activation, L-selectin is rapidly cleaved from the lymphocyte surface predominantly by the metalloprotease ADAM17. This loss of L-selectin is thought to prevent effector cells from homing to peripheral lymph nodes thereby indirectly promoting their trafficking to peripheral sites, although this has not yet been shown experimentally (von Andrian and Mackay, 2000). The molecules that regulate L-selectin shedding are still under investigation and include calmodulin, ERM proteins, and protein kinase C (Ivetic, 2013).

[1]Department of Immunology and Pathology, Monash University, Alfred Research Alliance, Melbourne, VIC 3004, Australia

[2]Centre for Inflammatory Diseases, Monash University Department of Medicine, Monash Medical Centre, 246 Clayton Road, Clayton, VIC 3168, Australia

[3]Radboud Institute for Molecular Life Sciences, Radboud University Medical Center, Nijmegen, The Netherlands

[4]Department of Biochemistry and Genetics, La Trobe Institute for Molecular Sciences, La Trobe University, Bundoora, VIC 3086, Australia

[5]Molecular Immunology, German Cancer Research Center, Heidelberg, Germany

[6]Institute of Translational Medicine, Faculty of Health Sciences, University of Macau, Taipa, Macau SAR, China

[7]Institute of Infection and Immunity, School of Medicine, Cardiff University, Cardiff CF14 4XN, UK

[8]Lead Contact

*Correspondence: mark.wright@monash.edu

https://doi.org/10.1016/j.isci.2020.101104

Tetraspanins are four-transmembrane proteins that play a key role in the molecular organization of cellular membranes. There are 34 tetraspanins encoded by the human genome, and these molecules interact with and organize their partner proteins into signal-transducing microdomains (Rubinstein et al., 2013). In immune cells, the tetraspanin molecular partners include integrins, immunoreceptors, and signaling molecules; thus, tetraspanins control key processes such as immune cell adhesion, migration, and activation (Jones et al., 2011; Yeung et al., 2018). The functions of many of the immune cell-expressed tetraspanins are now well documented. For example, in B cells, the tetraspanin CD81 promotes adhesion strengthening of α4β1 integrin (Feigelson et al., 2003) and additionally serves as a key component of the CD19/CD21 co-receptor complex that lowers the threshold of B cell signaling (van Zelm et al., 2010). In dendritic cells, CD81 (Quast et al., 2011) and the tetraspanins CD37 and CD82 (Gartlan et al., 2013; Jones et al., 2016) regulate the cytoskeletal rearrangements that drive migration. CD37 is also required for integrin function, both in neutrophils where it is required for inflammation-associated recruitment (Wee et al., 2015) and in B cells where it is essential for transducing survival signals during the germinal center reaction (van Spriel et al., 2012).

By contrast, the function of the pan-leukocyte marker CD53 remains obscure. Despite being one of the first discovered members of the tetraspanin superfamily (Amiot, 1990), CD53 has not been robustly examined, with a range of *in vitro* studies weakly suggesting a variety of roles. Cross-linking CD53 at the cell surface can lead to leukocyte activation (Bell et al., 1992; Bosca and Lazo, 1994; Cao et al., 1997; Lagaudriere-Gesbert et al., 1997; Lazo et al., 1997), a result perhaps explained by more recent sophisticated analyses that demonstrate a role for CD53 in PKC signaling (Zuidscherwoude et al., 2017). Transfection and expression studies have suggested a role in the regulation of apoptosis (Kim et al., 2004; Yunta and Lazo, 2003) and T cell development (Puls et al., 2002), whereas genetic and phenotypic analyses suggest a role for mutations in CD53 in immunodeficiency (Mollinedo et al., 1997) or various inflammatory disorders including arthritis, asthma, and Sjögren's syndrome (Bos et al., 2010; Khuder et al., 2015; Lee et al., 2013; Pedersen-Lane et al., 2007; Xu et al., 2015). Here, we analyze CD53 function using a reverse genetics approach. The data show a striking phenotype as CD53-deficient lymphocytes home poorly to lymph nodes, an effect associated with marked reductions in L-selectin expression and stability of these cells. Thus, we demonstrate that CD53 is a key player in the regulation of lymphocyte recirculation.

RESULTS AND DISCUSSION

The Cellularity of *Cd53*$^{-/-}$ Peripheral Lymph Nodes Is Reduced due to a Striking Defect in Lymphocyte Homing

To investigate the function of the tetraspanin CD53, we first analyzed the lymphoid organs of *Cd53*$^{-/-}$ mice. No difference in the gross appearance or mass of spleens was observed; however, *Cd53*$^{-/-}$ peripheral lymph nodes (pLN; inguinal and brachial) were smaller in appearance and weighed less than their wild-type (WT) counterparts (Figure 1A). CD53 ablation had no significant effect on the cellularity of the bone marrow, thymus, blood, spleen, and mesenteric lymph nodes. However, pLN from *Cd53*$^{-/-}$ mice showed a striking defect in cellularity with a reduction of approximately 60% compared with WT (Figure 1B). This was not a delay in development, as the cellularity in the spleens of WT and *Cd53*$^{-/-}$ mice was identical over time, whereas the pLN of *Cd53*$^{-/-}$ mice remained smaller even in 52-week-old mice (Figure 1C). To further analyze the impaired cellularity of *Cd53*$^{-/-}$ pLN, cells from pLN and spleen were analyzed by flow cytometry and lymphocytes were enumerated. Dot plot analyses showed a slight increase in the frequency of T cells and a striking reduction in the frequency of B cells in the pLN of *Cd53*$^{-/-}$ mice (Figure 1D). Quantification of absolute B cell numbers confirmed this reduction (Figure 1F). The number of pLN B cells in *Cd53*$^{-/-}$ mice was only ~14% of that in WT. For pLN T cells, quantification revealed a smaller, ~50% deficit, applying to both the CD4^{+} and CD8^{+} lineages. In parallel we observed a marginal, although significant, increase in the number of T cells in the spleen (Figure 1E).

Given the normal cellularity of the spleen and other lymphoid organs, and the documented roles of tetraspanins in regulating cell migration and leukocyte trafficking (Yeung et al., 2018), we reasoned that a defect in lymphocyte recirculation may underlie the phenotype of poor lymph node cellularity. We therefore evaluated whether CD53 ablation affected lymphocyte homing to lymph nodes. First, to investigate whether CD53 ablation had an effect on lymph node architecture or on HEVs, homing assays were performed where WT splenocytes were labeled with carboxyfluorescein succinimidyl ester (CFSE) and adoptively transferred into WT and *Cd53*$^{-/-}$ mice (Figure 2A). Flow cytometric analysis was used to identify the relative frequency of adoptively transferred splenocytes in each organ (Figure 2B), and to distinguish B and T cells (data not

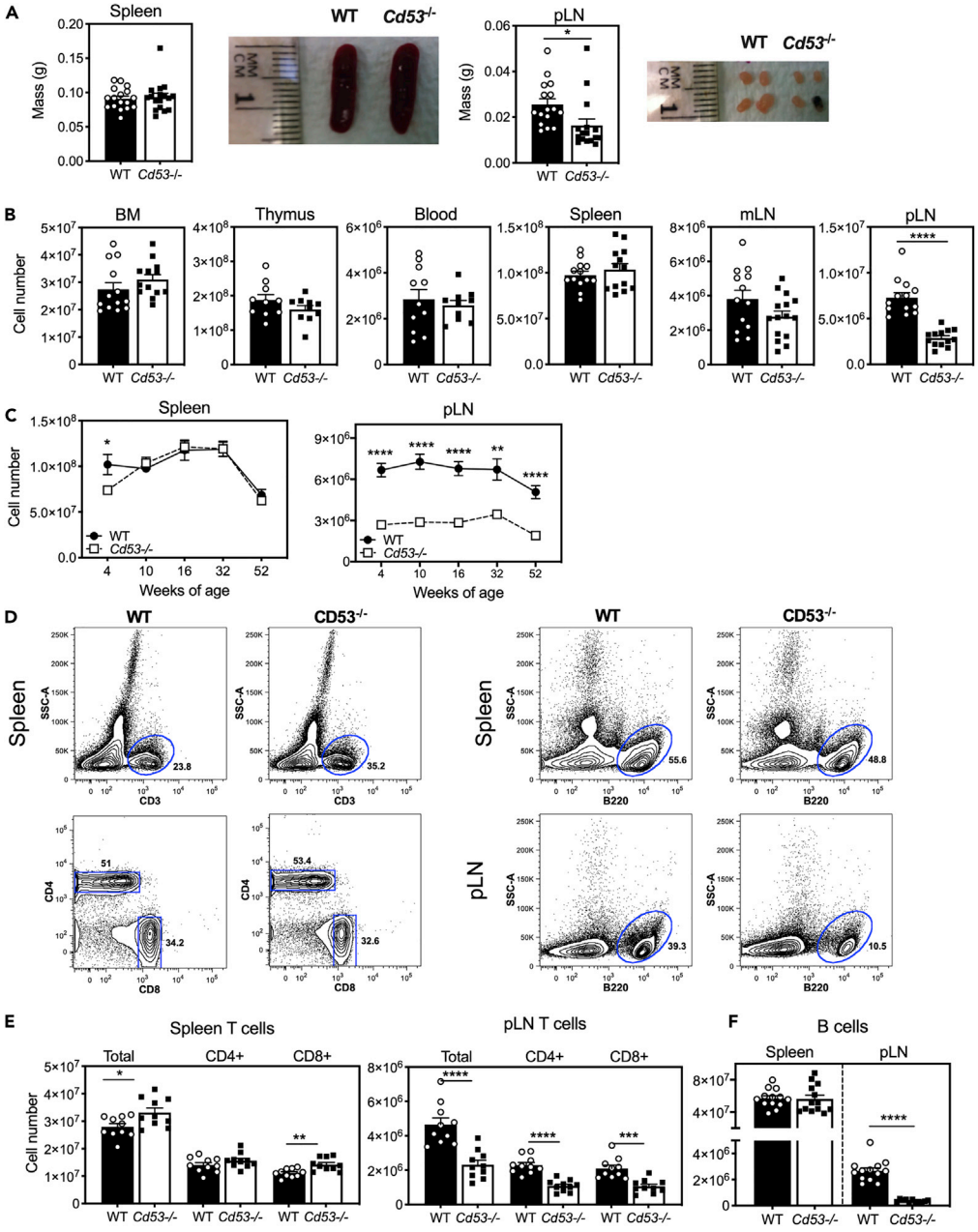

Figure 1. CD53 Ablation Reduces the Cellularity of Peripheral Lymph Nodes

Lymphoid organs from 10-week-old WT and *Cd53*$^{-/-}$ mice were harvested and analyzed.

(A) Representative images and mass of WT and *Cd53*$^{-/-}$ spleens and peripheral lymph nodes (pLN).

(B) Total cell numbers of lymphoid organs (BM, bone marrow; thymus; blood; spleen; mLN, mesenteric lymph nodes; and pLN).

(C) Total cell number of spleens and pLN as determined at time points from 4 to 52 weeks.

(D) Flow cytometry analyses of spleen and pLN identifying B (B220^{+}) and T (CD3^{+}) cells and CD4^{+} and CD8^{+} T cell populations.

(E and F) Quantification of (E) T cell and (F) B cell populations in spleen and pLN.

Data are represented as mean ± SEM, n = 6–17 mice per group pooled from 2–5 independent experiments, *p ≤ 0.05, **p ≤ 0.01, ***p ≤ 0.001, ****p ≤ 0.0001, Student's two-tailed unpaired t test.

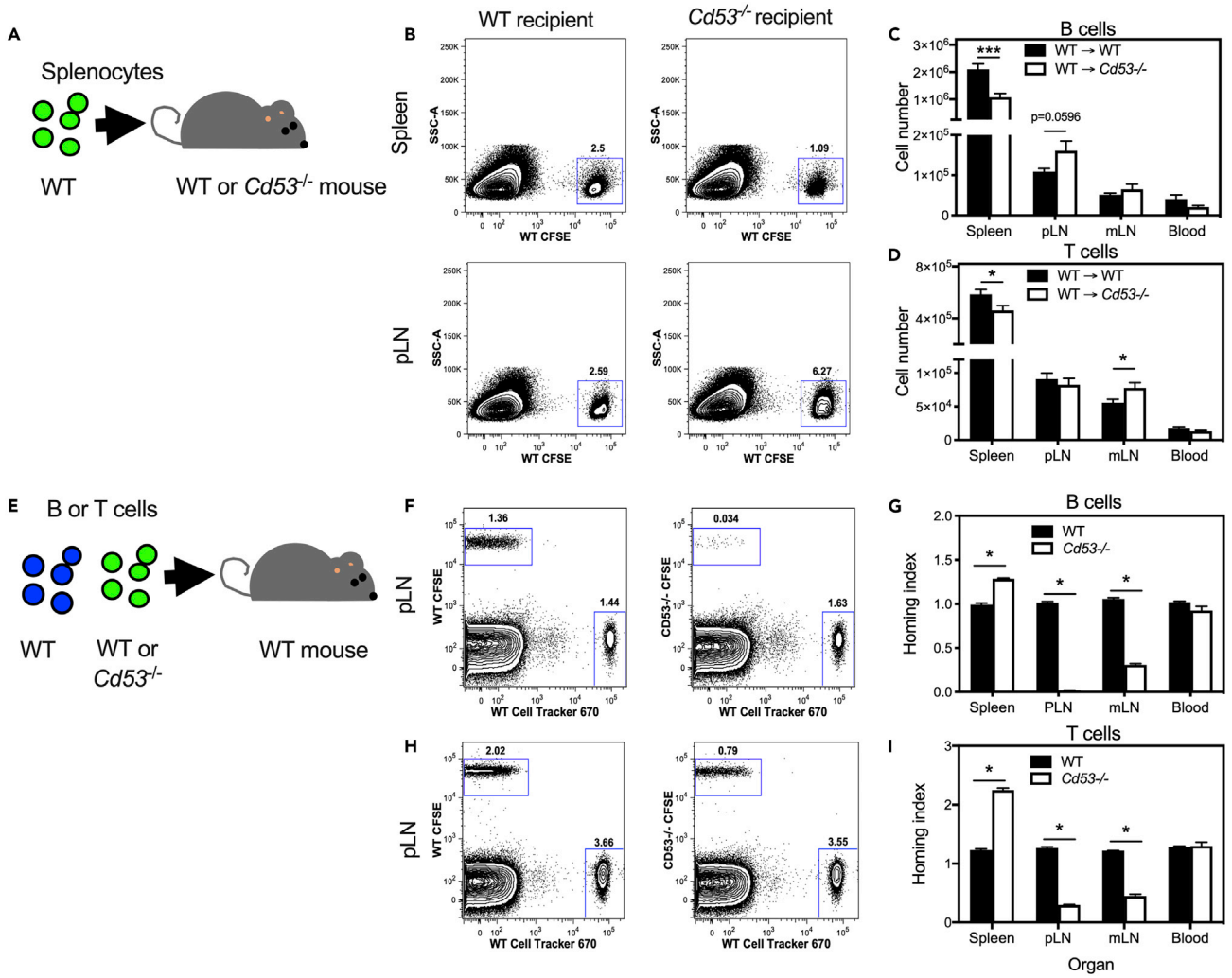

Figure 2. CD53 Is Required for Efficient Lymphocyte Homing to Lymph Nodes

(A–D) WT splenocytes were labeled with CFSE and injected intravenously (i.v.) into WT or *Cd53*$^{-/-}$ recipient mice. Forty-eight hours later lymphoid organs were harvested and analyzed for CFSE^{+} cells using flow cytometry. (A) Schematic, illustrating experimental design. (B) Representative flow cytometry illustrating the identification of transferred CFSE^{+} cells in the spleens and pLN of recipient mice. (C and D) Enumeration of CD19^{+}CFSE^{+} adoptively transferred B cells (C) and CD3^{+}CFSE^{+} adoptively transferred T cells (D) in the lymphoid organs of recipient mice. Data are from 8 mice per group pooled from 2 independent experiments.

(E–I) WT and *Cd53*$^{-/-}$ B or T cells were purified, CFSE-labeled, and co-injected i.v. into WT recipient mice together with an internal control of WT (B or T) cells differentially labeled with Cell Tracker 670. (E) Schematic, illustrating experimental design. (F and H) Representative flow cytometry comparing the homing of WT-Cell tracker 670^{+}, WT-CFSE^{+}, and *Cd53*$^{-/-}$CFSE^{+} CD19^{+} B cells (F) and CD3^{+} T cells (H) to peripheral lymph nodes. (G and I) Homing indices of transferred B cells (G) and T cells (I) to each organ.

Data are represented as mean + SEM, 8 mice per group pooled from 2 independent experiments, *p ≤ 0.05, ***p ≤ 0.001, Student's two-tailed unpaired t test (C and D) or Mann-Whitney test (G and I).

shown). The data clearly show that whereas there was an impairment in the ability of adoptively transferred WT B and T cells to home to the spleens of *Cd53*$^{-/-}$ mice, homing to peripheral and mesenteric lymph nodes was normal (Figures 2C and 2D). Thus, the reduced cellularity of *Cd53*$^{-/-}$ pLN is likely a phenotype intrinsic to *Cd53*$^{-/-}$ lymphocytes. Next, we investigated the homing capacity of *Cd53*$^{-/-}$ lymphocytes. WT and *Cd53*$^{-/-}$ B or T cells were purified, labeled with CFSE, and co-injected into WT recipient mice together with an internal control of WT (B or T) cells differentially labeled with Cell Tracker 670 (Figure 2E). After 48 h immune organs were harvested and homing analyzed by flow cytometry (Figures 2F and 2H). Quantification was calculated using a homing index (Arbones et al., 1994) where the ratio of CFSE^{+} test cells to Cell Tracker 670^{+} internal control cells in the initial injection mixture and also within each organ

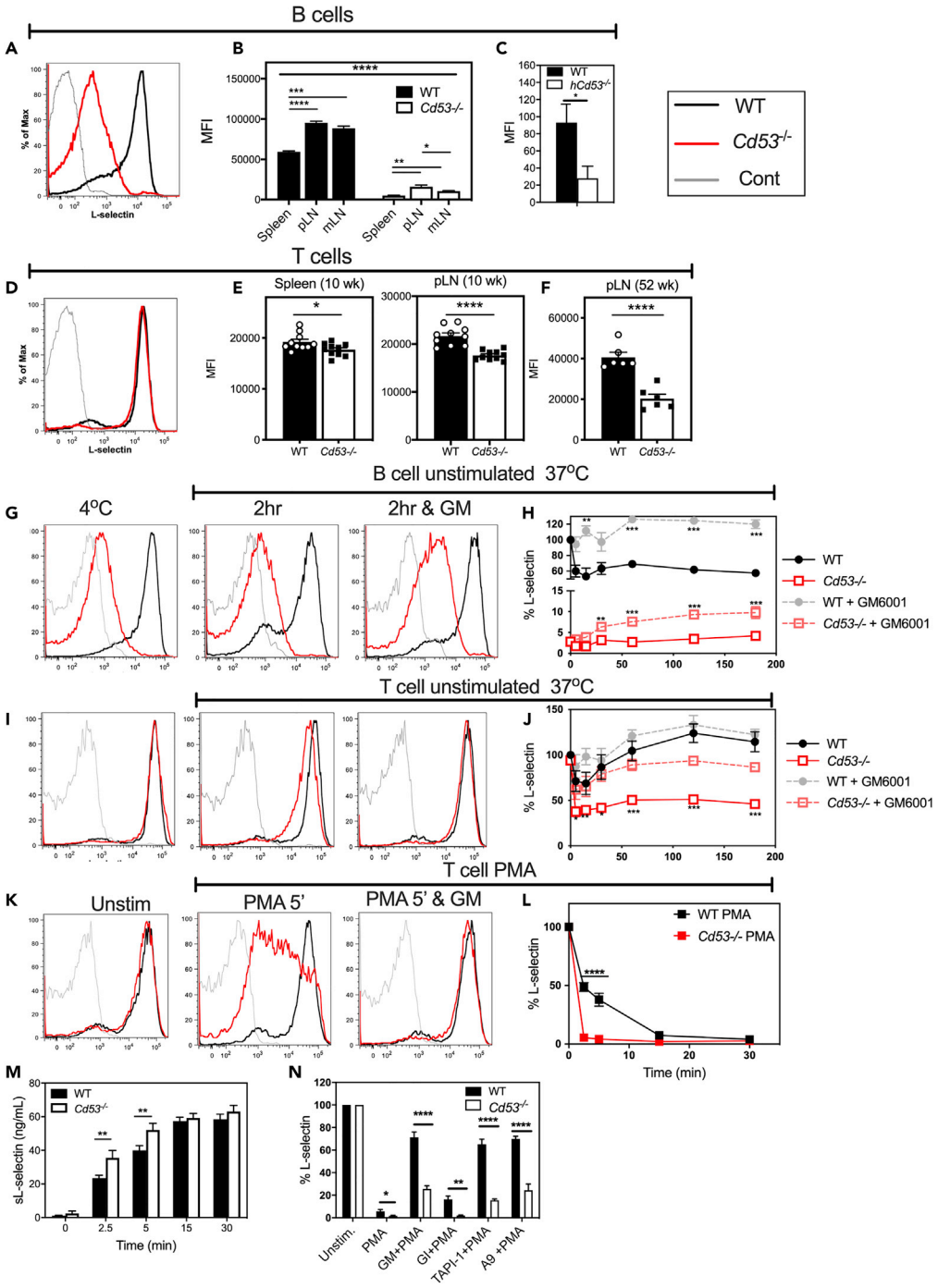

Figure 3. CD53 Stabilizes L-Selectin Expression on the Lymphocyte Surface

(A and B) (A) Representative flow cytometry histograms (splenic B cells), and quantification of L-selectin protein expression (B; mean fluorescent intensity, MFI) on B220^{+} WT and *Cd53*$^{-/-}$ B cells harvested from spleen, peripheral lymph nodes (pLN), and mesenteric lymph nodes (mLN). Data are represented as mean + SEM, 3 mice per group, representative of ≥3 independent experiments.

(C) Expression of WT human L-selectin on WT and *hCd53*$^{-/-}$ human BJAB cells.

(D and E) (D) Representative flow cytometry (splenic T cells) and quantification (E, MFI) of L-selectin expression on CD3^{+} WT and *Cd53*$^{-/-}$ T cells harvested from spleen and pLNs from 10-week-old mice. Data are represented as mean + SEM, 10 mice per group pooled from 2 independent experiments.

Figure 3. *Continued*

(F) Quantification of L-selectin expression (MFI) on $CD3^+$ T cells harvested from aged (52-week-old) WT and $Cd53^{-/-}$ mice. Data are represented as mean + SEM, n = 6 mice per group representative of 2 independent experiments.
(G–J) WT and $Cd53^{-/-}$ splenocytes were cultured at 37°C with or without the broad metalloprotease inhibitor GM6001 (GM; 100μM). Flow cytometry was used to distinguish B ($B220^+$) and T ($CD3^+$) cells and monitor L-selectin expression. (G and I) Representative flow cytometry histograms displaying L-selectin expression on B cells (G) and T cells (I) after 2 h at 37°C. (H and J) The kinetics of L-selectin expression on cultured B (H) and T (J) cells relative to cells held at 4°C.
(K–N) Purified WT and $Cd53^{-/-}$ T cells were stimulated with PMA (50 ng/mL) to induce shedding in the presence or absence of metalloprotease inhibitors. (K) Representative histograms illustrating L-selectin expression in unstimulated (unstim), PMA stimulated (5′), and PMA stimulated in the presence of the metalloprotease inhibitor GM6001 (PMA 5′ + GM). (L) The kinetics of L-selectin surface expression (relative to unstimulated cells) and (M) amount of soluble L-selectin shed into supernatants of WT and $Cd53^{-/-}$ T cells stimulated with PMA. (N) The percentage of L-selectin expression (relative to unstimulated cells) remaining after 15′ PMA stimulation in the presence or absence of the metalloprotease inhibitors GM6001 (100 μM, GM), GI 254023X (20 μM, GI), TAPI-1 (200 μM), and A9 (5 μM).
Data are represented as mean ± SEM, n = 6–7 mice per group pooled from 3 independent experiments, *p ≤ 0.05, **p ≤ 0.01, ***p ≤ 0.001, ****p ≤ 0.0001, Student's two-tailed unpaired t test (B, C, E, F, M, N) or Mann-Whitney test (H, J, L). See also Figures S1–S3.

was determined (Figures 2G and 2I). For B cells, *Cd53* deficiency resulted in a striking defect (Figure 2F). Although $Cd53^{-/-}$ B cells were able to localize to blood normally, they preferentially localized to the spleen, whereas homing to the pLN was almost completely abrogated (Figure 2G). There was also a significant reduction of B cell homing to the mesenteric lymph nodes (25% of WT; Figure 2G). A similar dysregulation in $Cd53^{-/-}$ T cell lymph node homing was observed, although the phenotype was not as pronounced (Figure 2H). $Cd53^{-/-}$ T cells also preferentially localized to the spleen, whereas homing to both the pLN and mLN was poor (Figure 2I). In conclusion, CD53 ablation induces reduced cellularity in pLN due to a severe defect in lymphocyte homing, with the phenotype more pronounced in B cells than in T cells.

CD53 Ablation Impairs Expression of L-Selectin on Lymphocytes

Given that CD53 ablation induces a defect in lymph node homing, we hypothesized that CD53 might regulate the key lymph node homing receptor, L-selectin. We therefore analyzed L-selectin expression by flow cytometry and identified that the residual B cell ($B220^+$) population found in $Cd53^{-/-}$ pLN had significantly reduced expression of L-selectin protein (Figure 3A). Indeed, across spleen, pLN, and mLN there was a major reduction in the surface expression of L-selectin on $Cd53^{-/-}$ B cells of up to two orders of magnitude (Figure 3B). To investigate whether our findings extended to human cells, we generated human $Cd53^{-/-}$ B cell lines (BJAB) using CRISPR/Cas9 technology. We observed impaired cell surface L-selectin expression in two independent human $Cd53^{-/-}$ B cell lines, in accord with our mouse data (Figure 3C). In comparison, the expression of L-selectin on $Cd53^{-/-}$ T cells revealed a small, but significant, reduction of L-selectin expression of 8% and 20% in splenic and pLN T cells, respectively (Figures 3D and 3E). This diminution of L-selectin expression was exaggerated in T cells from aged mice where there was an approximately 60% reduction of L-selectin expression (Figure 3F).

To investigate the mechanism by which CD53 regulates L-selectin we first analyzed mRNA expression in lymphocytes and could detect no reduction in L-selectin mRNA expression associated with CD53 ablation in both resting and activated cells (Figure S1). L-selectin is cleaved from the surface of lymphocytes by metalloproteases. In activated lymphocytes, the predominant metalloprotease that drives shedding is ADAM17, whereas the metalloprotease responsible for the constitutive shedding observed in unactivated lymphocytes has not been identified (Mohammed et al., 2019). There is growing evidence that tetraspanins can regulate this enzyme family. For example, the TspanC8 subgroup of tetraspanins molecularly interacts with and regulates the activity of ADAM10 (Matthews et al., 2017). We therefore investigated whether CD53 regulates L-selectin expression via effects on metalloproteases. We first examined L-selectin expression on unstimulated WT and $Cd53^{-/-}$ B cells incubated at 37°C in the presence of the broad-spectrum matrix metalloprotease inhibitor, GM6001. Incubation of WT B cells at 37°C induced a spontaneous reduction in L-selectin expression, which was completely inhibited by GM6001 (Figure 3H). L-selectin expression on $Cd53^{-/-}$ B cells was much lower than on WT cells, and although incubation of $Cd53^{-/-}$ B cells with GM6001 (Figures 3G and 3H) increased L-selectin expression more than 3-fold, it could not restore expression to WT levels. This suggests that the reduced L-selectin expression on $Cd53^{-/-}$ B cells may be only partially accounted for by metalloproteinase activity. Incubation of WT T cells at 37°C also induced a spontaneous reduction in L-selectin expression, and this reduction was significantly exaggerated in $Cd53^{-/-}$ T cells (Figures 3I and 3J). In marked contrast to B cells, the reduced levels of L-selectin on $CD53^{-/-}$

T cells were substantially restored up to ~80% of WT levels by GM6001. This finding suggests that the lower levels of L-selectin in CD53$^{-/-}$ T cells are largely due to spontaneous shedding. To study the impact of CD53 on ADAM-17-dependent L-selectin shedding in T cells, we used phorbol 12-myrsitate 13-acetate (PMA) activation. We observed that the reduction of L-selectin surface expression from *Cd53*$^{-/-}$ T cells was significantly accelerated (Figures 3K and 3L), with an increase in shed soluble L-selectin levels observed in the supernatant of *Cd53*$^{-/-}$ when compared with WT cells (Figure 3M). GM6001 and TAPI-1 (another small molecule metalloprotease inhibitor that can inhibit ADAM17) were able to largely prevent the loss of L-selectin surface expression in WT T cells and maintain L-selectin at ~70% of unstimulated levels, whereas these inhibitors were all less effective in PMA-stimulated *Cd53*$^{-/-}$ T cells and could only maintain L-selectin expression at ~25% of unstimulated levels. Similarly, the ADAM-17 blocking monoclonal antibody A9 (Kwok et al., 2014) was also less effective in inhibiting PMA-induced reduction of L-selectin surface expression on *Cd53*$^{-/-}$ T cells compared with WT T cells. The ADAM-10-specific inhibitor GI254023X had no effect in these assays (Figure 3N), demonstrating that ADAM10 did not substitute for ADAM-17 in PMA-activated T cells as shown here and by others (Mohammed et al., 2019).

In summary, treatment with metalloprotease inhibitors: increases the expression of L-selectin on *Cd53*$^{-/-}$ B cells (Figures 3G and 3H), prevents the instability of L-selectin expression on *Cd53*$^{-/-}$ T cells (Figures 3I and 3J), and partially restores L-selectin expression in PMA-treated *Cd53*$^{-/-}$ T cells (Figures 3K and 3N). Taken with the exaggerated accumulation of L-selectin in the supernatant of PMA-activated *Cd53*$^{-/-}$ T cells (at early time points, Figure 3M), the data support a role for CD53 in inhibiting metalloprotease-mediated shedding of L-selectin from the lymphocyte surface. However, analyses of ADAM17-deficient cells and mice indicate that there are additional mechanisms of regulating L-selectin expression and shedding that are independent of ADAM17 (Le Gall et al., 2009; Walcheck et al., 2003; Wang et al., 2010). Given that metalloprotease inhibitors, or a blocking antibody targeting ADAM17, diminished but did not abrogate the excessive loss of L-selectin induced by PMA stimulation on the surface of *Cd53*$^{-/-}$ T cells, our data indicate that CD53 also inhibits ADAM17-independent mechanisms, some of which may be metalloprotease-independent. One possibility is that CD53 might have a role in L-selectin trafficking. We therefore distinguished intracellular and extracellular L-selectin expression in resting and PMA-activated permeabilized lymphocytes, but could detect no evidence of an intracellular accumulation of L-selectin in *Cd53*$^{-/-}$ cells, arguing against a role for CD53 in either trafficking L-selectin to the cell surface or internalizing L-selectin after activation (Figure S2). Taken together, we conclude that CD53 is required to stabilize L-selectin expression at the lymphocyte surface, and further studies will be required to identify the additional metalloprotease(s) or mechanisms responsible.

Cd53$^{-/-}$ B cells express very low levels of L-selectin, and consequently are unable to home to peripheral lymph nodes. By contrast, L-selectin expression in *Cd53*$^{-/-}$ T cells is only marginally reduced (Figure 3) but is unstable, as shown by the relatively poor expression of L-selectin on T cells from aged *Cd53*$^{-/-}$ mice (Figure 3F), and the spontaneous loss of L-selectin surface expression induced by incubation of *Cd53*$^{-/-}$ T cells at 37°C (Figures 3I and 3J). This L-selectin instability likely explains the impairment of *Cd53*$^{-/-}$ T cell homing to peripheral lymph nodes, although we cannot rule out other mechanisms such as a defect in signal transduction. In line with this, we have recently shown that CD53 can directly interact with PKC and is required for PKC activation in B cells (Zuidscherwoude et al., 2017), suggesting that CD53 interacts with PKC and L-selectin in the same molecular complex (Kilian et al., 2004). The difference in the biology of CD53 ablation on B and T cells likely reflects the ratio of CD53:L-selectin expression on the two cell types. CD53 is expressed at higher levels on B cells than on T cells (Tomlinson et al., 1995), whereas T cells express approximately 50% more L-selectin than do B cells (Gauguet et al., 2004). Thus, on B cells there is relatively more CD53 available to stabilize lower levels of L-selectin (and vice versa). Alternatively, there may be another tetraspanin that compensates for CD53 on T cells, but is not expressed in B cells. One candidate is CD9, as *in vitro* studies have shown that it can inhibit ADAM17-mediated shedding of another substrate, tumor necrosis factor (Gutierrez-Lopez et al., 2011), and it is strongly expressed on T cells but not on most B cells. However, we think this is unlikely as lymph node cellularity in *Cd9*$^{-/-}$ mice is normal (Iwasaki et al., 2013) and CD53 ablation does not significantly affect CD9 expression in either *Cd53*$^{-/-}$ T cells or *hCd53*$^{-/-}$ BJAB cells (Figure S3).

Defective Lymphocyte Homing Delays Adaptive Immune Responses when Antigen Is Delivered to Lymph Nodes

To examine whether the impairment of lymphocyte recirculation in *Cd53*$^{-/-}$ mice had an effect on immunity, mice were first challenged with classical model antigens (namely the type I T-independent

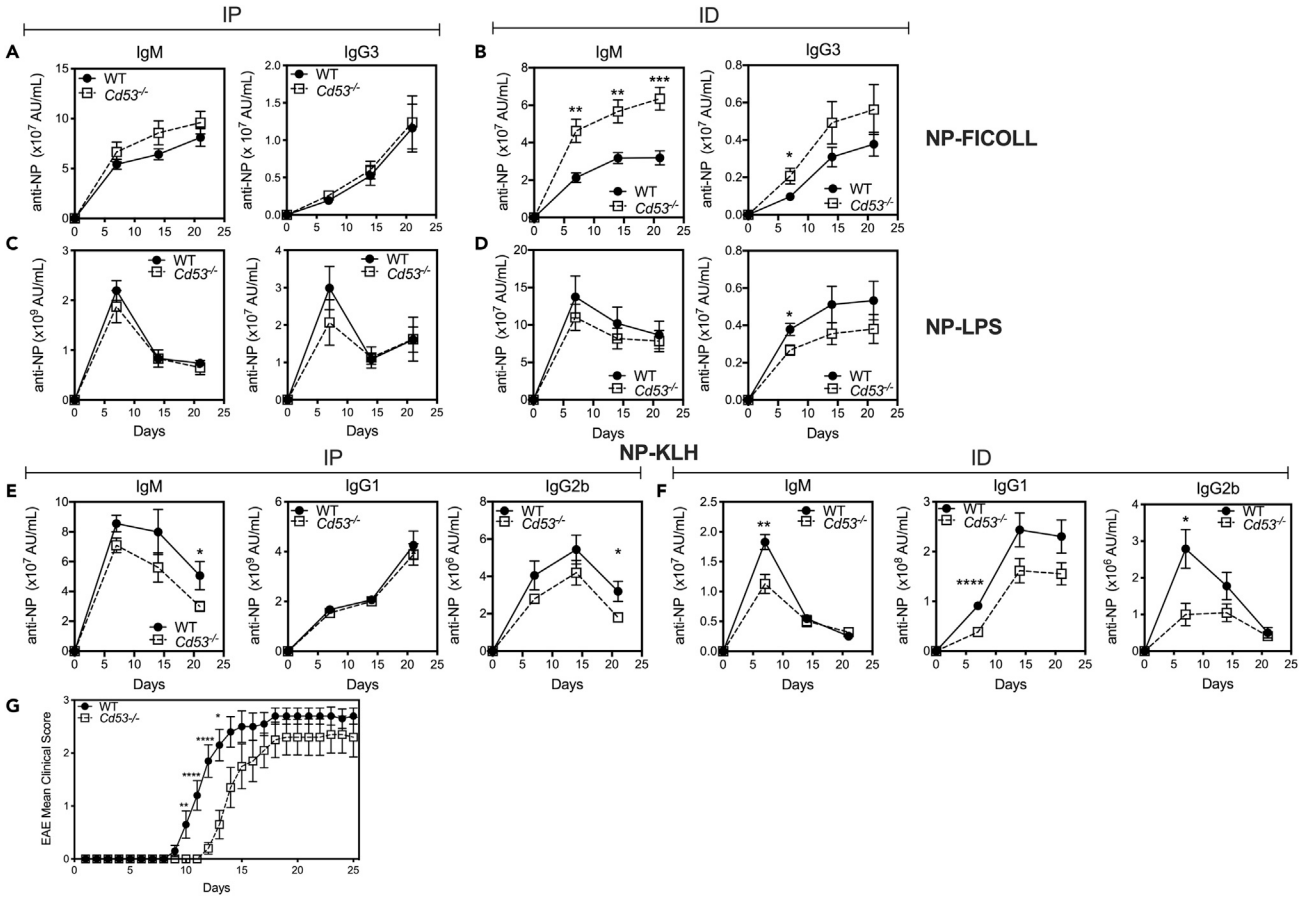

Figure 4. Adaptive Immune Responses in *Cd53*$^{-/-}$ Mice Are Delayed when Antigen Is Delivered to Lymph Nodes

(A–F) WT and *Cd53*$^{-/-}$ mice were immunized intraperitoneally (IP; A, C, and E) or intradermally (ID; B, D, and F) with (A and B) 50 μg NP-FICOLL, (C and D) 50 μg NP-LPS, or (E and F) 50 μg NP-KLH. NP-specific antibody responses were determined by ELISA for IgM, IgG1, IgG2b, and IgG3. Data are represented as mean ± SEM, 9–17 mice per group pooled from 2 independent experiments.

(G) Autoimmune encephalomyelitis was induced in WT and *Cd53*$^{-/-}$ mice where mice were immunized subcutaneously with MOG peptide. Disease progression was measured daily and expressed as a clinical score as mean ± SEM, 10 mice per group from 2 independent experiments. *p ≤ 0.05, **p ≤ 0.01, ***p ≤ 0.001, ****p ≤ 0.0001, Student's two-tailed unpaired t test (A–F) or two-way ANOVA (G).

antigen NP-LPS, the type II T-independent antigen NP-FICOLL, and the classical T-dependent antigen NP-KLH) to induce humoral responses. Antibody responses of *Cd53*$^{-/-}$ mice were largely normal to all antigens administered systemically (intraperitoneally, Figures 4A, 4C, and 4E). Similarly, responses to intradermal NP-LPS were also normal (Figure 4D). Collectively, these data indicate that CD53 ablation does not significantly affect the germinal center reaction, antigen presentation, T cell help, or the ability of B cells to proliferate and generate plasma cells. However, when NP-KLH was delivered to lymph nodes via intradermal injection, *Cd53*$^{-/-}$ antibody responses were significantly delayed (Figure 4F). Similarly, with regard to T cell responses, the clinical responses of *Cd53*$^{-/-}$ mice in experimental autoimmune encephalomyelitis, a T cell-dependent model of autoimmunity initiated by subcutaneous immunization with MOG peptide, were also delayed (Figure 4G). We conclude that when antigen is delivered to the lymph nodes of *Cd53*$^{-/-}$ mice adaptive immune responses are delayed. This pattern of normal responses to systemically administered antigen versus delayed immunity when antigen is delivered to pLN via the subcutaneous and intradermal routes is strikingly similar to that reported for L-selectin knockout mice (Catalina et al., 1996; Steeber et al., 1996). This illustrates the importance of lymphocyte recirculation in immunity; presumably, the poor cellularity of lymphocytes, particularly B cells, in the lymph node delays immune responses. The one exception here was the exaggerated immune responses of *Cd53*$^{-/-}$ mice to NP-FICOLL when administered intradermally (Figure 4B). It is difficult to explain this result, although this was also observed in L-selectin-deficient mice (Steeber et al., 1996). T-independent type II antigen responses arise in the marginal zone of the spleen

where marginal zone B cells, B1 cells, and splenic macrophages are all thought to play a critical role (Vinuesa and Chang, 2013). The numbers of these cell populations are normal in *Cd53*$^{-/-}$ mice, and we can only speculate either that a deficiency in the CD53/L-selectin axis induces subtle changes in trafficking or localization in these populations or that L-selectin expressed in these populations has a hitherto undiscovered function in negatively regulating type II T-independent responses.

In summary, these analyses identify an indispensable role for CD53 in maintaining lymph node cellularity (Figure 1). A very recent analysis of *Cd53*$^{-/-}$ mice attributed the poor lymph node cellularity to defects in B cell development and showed evidence that CD53 is required for optimal interleukin-7R signaling (Greenberg et al., 2020). Here we identify another mechanism: CD53 is required for lymphocyte homing to lymph nodes (Figure 2). The central role of L-selectin in lymph node homing is well established. However, the molecular mechanisms underlying L-selectin stabilization at the plasma membrane are less well understood. This article demonstrates that L-selectin expression on lymphocytes is tightly controlled by the leukocyte-specific tetraspanin CD53 and that CD53, at least partially, mediates this effect by inhibiting L-selectin shedding (Figure 3). Consequently, CD53 is required for efficient and timely immune responses (Figure 4).

Limitations of This Study

This article analyzes the development and immune responses of *Cd53*$^{-/-}$ mice and the immunobiology of *Cd53*$^{-/-}$ lymphocytes in *in vivo* and *in vitro* assays. The molecular interactions of CD53 and the mechanisms by which it stabilizes L-selectin surface expression await further analyses.

Resource Availability

Lead Contact

Further information and requests should be directed to and will be fulfilled by the Lead Contact, Mark Wright (mark.wright@monash.edu).

Materials Availability

All materials are available from the lead contact upon reasonable request, but we may require a materials transfer agreement.

Data and Code Availability

The data that support the findings of this paper are available from the lead contact upon reasonable request.

METHODS

All methods can be found in the accompanying Transparent Methods supplemental file.

SUPPLEMENTAL INFORMATION

Supplemental Information can be found online at https://doi.org/10.1016/j.isci.2020.101104.

ACKNOWLEDGMENTS

This work was supported by the National Health and Medical Research Council (NHMRC), Australia (Senior Research Fellowship ID 1042775 to M.J.H.). A.v.S. is supported by the Netherlands Organisation for Scientific Research (Gravitation Program ICI-024.002.009), the Dutch Cancer Society (KUN2014-6845), and the European Research Council (Consolidator Grant 724281). H.F.K. was supported by the Science and Technology Development Fund, Macau SAR (File no. 005/2019/A1).

AUTHOR CONTRIBUTIONS

M.C.D., L.Y., R.P., J.L.W., M.M., E.L.J., Z.N., F.A., P.H., B.C.S., A.v.S., M.J.H., and M.D.W. designed, performed, and analyzed experiments. G.H. generated the *Cd53*$^{-/-}$ mice. A.A. and A.N. generated L-selectin expression constructs and designed experiments incorporating their use. H.F.K. generated inhibitory ADAM17 mAbs and advised on their use. M.C.D., F.A., K.J.B, A.v.S., A.A., M.J.H., and M.D.W. wrote and edited the manuscript.

DECLARATION OF INTERESTS

The authors declare no competing interests.

Received: November 1, 2019
Revised: February 14, 2020
Accepted: April 23, 2020
Published: May 22, 2020

REFERENCES

Alanio, C., Lemaitre, F., Law, H.K., Hasan, M., and Albert, M.L. (2010). Enumeration of human antigen-specific naive CD8+ T cells reveals conserved precursor frequencies. Blood *115*, 3718–3725.

Amiot, M. (1990). Identification and analysis of cDNA clones encoding CD53. A pan-leukocyte antigen related to membrane transport proteins. J. Immunol. *145*, 4322–4325.

Arbones, M.L., Ord, D.C., Ley, K., Ratech, H., Maynard-Curry, C., Otten, G., Capon, D.J., and Tedder, T.F. (1994). Lymphocyte homing and leukocyte rolling and migration are impaired in L-selectin-deficient mice. Immunity *1*, 247–260.

Bell, G.M., Seaman, W.E., Niemi, E.C., and Imboden, J.B. (1992). The OX-44 molecule couples to signalling pathways and is associated with CD2 on rat T lymphocytes and a natural killer cell line. J. Exp. Med. *175*, 527–536.

Bos, S.D., Lakenberg, N., van der Breggen, R., Houwing-Duistermaat, J.J., Kloppenburg, M., de Craen, A.J., Beekman, M., Meulenbelt, I., and Slagboom, P.E. (2010). A genome-wide linkage scan reveals CD53 as an important regulator of innate TNF-alpha levels. Eur. J. Hum. Genet. *18*, 953–959.

Bosca, L., and Lazo, P.A. (1994). Induction of nitric oxide release by MRC OX-44 (anti-CD53) through a protein kinase C-dependent pathway in rat macrophages. J. Exp. Med. *179*, 1119–1126.

Cao, L., Yoshino, T., Kawasaki, N., Sakuma, I., Takahashi, K., and Akagi, T. (1997). Anti-CD53 monoclonal antibody induced LFA-1/ICAM-1-dependent and -independent lymphocyte homotypic cell aggregation. Immunobiology *197*, 70–81.

Catalina, M.D., Carroll, M.C., Arizpe, H., Takashima, A., Estess, P., and Siegelman, M.H. (1996). The route of antigen entry determines the requirement for L-selectin during immune responses. J. Exp. Med. *184*, 2341–2351.

Chu, H.H., Moon, J.J., Takada, K., Pepper, M., Molitor, J.A., Schacker, T.W., Hogquist, K.A., Jameson, S.C., and Jenkins, M.K. (2009). Positive selection optimizes the number and function of MHCII-restricted CD4+ T cell clones in the naive polyclonal repertoire. Proc. Natl. Acad. Sci. U S A *106*, 11241–11245.

Feigelson, S.W., Grabovsky, V., Shamri, R., Levy, S., and Alon, R. (2003). The CD81 tetraspanin facilitates instantaneous leukocyte VLA-4 adhesion strengthening to vascular cell adhesion molecule 1 (VCAM-1) under shear flow. J. Biol. Chem. *278*, 51203–51212.

Gartlan, K.H., Wee, J.L., Demaria, M.C., Nastovska, R., Chang, T.M., Jones, E.L., Apostolopoulos, V., Pietersz, G.A., Hickey, M.J., van Spriel, A.B., et al. (2013). Tetraspanin CD37 contributes to the initiation of cellular immunity by promoting dendritic cell migration. Eur. J. Immunol. *43*, 1208–1219.

Gauguet, J.M., Rosen, S.D., Marth, J.D., and von Andrian, U.H. (2004). Core 2 branching beta1,6-N-acetylglucosaminyltransferase and high endothelial cell N-acetylglucosamine-6-sulfotransferase exert differential control over B- and T-lymphocyte homing to peripheral lymph nodes. Blood *104*, 4104–4112.

Gowans, J.L. (1959). The recirculation of lymphocytes from blood to lymph in the rat. J. Physiol. *146*, 54–69.

Grailer, J.J., Kodera, M., and Steeber, D.A. (2009). L-selectin: role in regulating homeostasis and cutaneous inflammation. J. Dermatol. Sci. *56*, 141–147.

Greenberg, Z.J., Monlish, D.A., Bartnett, R.L., Yang, Y., Shen, G., Li, W., Bednarski, J.J., and Schuettpelz, L.G. (2020). The tetraspanin CD53 regulates early B cell development by promoting IL-7R signaling. J. Immunol. *204*, 58–67.

Gutierrez-Lopez, M.D., Gilsanz, A., Yanez-Mo, M., Ovalle, S., Lafuente, E.M., Dominguez, C., Monk, P.N., Gonzalez-Alvaro, I., Sanchez-Madrid, F., and Cabanas, C. (2011). The sheddase activity of ADAM17/TACE is regulated by the tetraspanin CD9. Cell Mol. Life Sci. *68*, 3275–3292.

Ivetic, A. (2013). Signals regulating L-selectin-dependent leucocyte adhesion and transmigration. Int. J. Biochem. Cell Biol. *45*, 550–555.

Iwasaki, T., Takeda, Y., Maruyama, K., Yokosaki, Y., Tsujino, K., Tetsumoto, S., Kuhara, H., Nakanishi, K., Otani, Y., Jin, Y., et al. (2013). Deletion of tetraspanin CD9 diminishes lymphangiogenesis in vivo and in vitro. J. Biol. Chem. *288*, 2118–2131.

Jones, E.L., Demaria, M.C., and Wright, M.D. (2011). Tetraspanins in cellular immunity. Biochem. Soc. Trans. *39*, 506–511.

Jones, E.L., Wee, J.L., Demaria, M.C., Blakeley, J., Ho, P.K., Vega-Ramos, J., Villadangos, J.A., van Spriel, A.B., Hickey, M.J., Hammerling, G.J., et al. (2016). Dendritic cell migration and antigen presentation are coordinated by the opposing functions of the tetraspanins CD82 and CD37. J. Immunol. *196*, 978–987.

Khuder, S.A., Al-Hashimi, I., Mutgi, A.B., and Altorok, N. (2015). Identification of potential genomic biomarkers for Sjogren's syndrome using data pooling of gene expression microarrays. Rheumatol. Int. *35*, 829–836.

Kilian, K., Dernedde, J., Mueller, E.C., Bahr, I., and Tauber, R. (2004). The interaction of protein kinase C isozymes alpha, iota, and theta with the cytoplasmic domain of L-selectin is modulated by phosphorylation of the receptor. J. Biol. Chem. *279*, 34472–34480.

Kim, T.R., Yoon, J.H., Kim, Y.C., Yook, Y.H., Kim, I.G., Kim, Y.S., Lee, H., and Paik, S.G. (2004). LPS-induced CD53 expression: a protection mechanism against oxidative and radiation stress. Mol. Cell *17*, 125–131.

Kwok, H.F., Botkjaer, K.A., Tape, C.J., Huang, Y., McCafferty, J., and Murphy, G. (2014). Development of a 'mouse and human cross-reactive' affinity-matured exosite inhibitory human antibody specific to TACE (ADAM17) for cancer immunotherapy. Protein Eng. Des. Sel. *27*, 179–190.

Lagaudriere-Gesbert, C., Le Naour, F., Lebel-Binay, S., Billard, M., Lemichez, E., Boquet, P., Boucheix, C., Conjeaud, H., and Rubinstein, E. (1997). Functional analysis of four tetraspans, CD9, CD53, CD81, and CD82, suggests a common role in costimulation, cell adhesion, and migration: only CD9 upregulates HB-EGF activity. Cell Immunol. *182*, 105–112.

Lazo, P.A., Cuevas, L., Gutierrez del Arroyo, A., and Orue, E. (1997). Ligation of CD53/OX44, a tetraspan antigen, induces homotypic adhesion mediated by specific cell-cell interactions. Cell Immunol. *178*, 132–140.

Le Gall, S.M., Bobe, P., Reiss, K., Horiuchi, K., Niu, X.D., Lundell, D., Gibb, D.R., Conrad, D., Saftig, P., and Blobel, C.P. (2009). ADAMs 10 and 17 represent differentially regulated components of a general shedding machinery for membrane proteins such as transforming growth factor alpha, L-selectin, and tumor necrosis factor alpha. Mol. Biol. Cell *20*, 1785–1794.

Lee, H., Bae, S., Jang, J., Choi, B.W., Park, C.S., Park, J.S., Lee, S.H., and Yoon, Y. (2013). CD53, a suppressor of inflammatory cytokine production, is associated with population asthma risk via the functional promoter polymorphism -1560 C>T. Biochim. Biophys. Acta *1830*, 3011–3018.

Matthews, A.L., Szyroka, J., Collier, R., Noy, P.J., and Tomlinson, M.G. (2017). Scissor sisters: regulation of ADAM10 by the TspanC8 tetraspanins. Biochem. Soc. Trans. *45*, 719–730.

Mohammed, R.N., Wehenkel, S.C., Galkina, E.V., Yates, E.K., Preece, G., Newman, A., Watson, H.A., Ohme, J., Bridgeman, J.S., Durairaj, R.R.P., et al. (2019). ADAM17-dependent proteolysis of

L-selectin promotes early clonal expansion of cytotoxic T cells. Sci. Rep. *9*, 5487.

Mollinedo, F., Fontan, G., Barasoain, I., and Lazo, P.A. (1997). Recurrent infectious diseases in human CD53 deficiency. Clin. Diagn. Lab Immunol. *4*, 229–231.

Moon, J.J., Chu, H.H., Pepper, M., McSorley, S.J., Jameson, S.C., Kedl, R.M., and Jenkins, M.K. (2007). Naive CD4(+) T cell frequency varies for different epitopes and predicts repertoire diversity and response magnitude. Immunity *27*, 203–213.

Obar, J.J., Khanna, K.M., and Lefrancois, L. (2008). Endogenous naive CD8+ T cell precursor frequency regulates primary and memory responses to infection. Immunity *28*, 859–869.

Pedersen-Lane, J.H., Zurier, R.B., and Lawrence, D.A. (2007). Analysis of the thiol status of peripheral blood leukocytes in rheumatoid arthritis patients. J. Leukoc. Biol. *81*, 934–941.

Puls, K.L., Hogquist, K.A., Reilly, N., and Wright, M.D. (2002). CD53, a thymocyte selection marker whose induction requires a lower affinity TCR-MHC interaction than CD69, but is up-regulated with slower kinetics. Int. Immunol. *14*, 249–258.

Quast, T., Eppler, F., Semmling, V., Schild, C., Homsi, Y., Levy, S., Lang, T., Kurts, C., and Kolanus, W. (2011). CD81 is essential for the formation of membrane protrusions and regulates Rac1-activation in adhesion-dependent immune cell migration. Blood *118*, 1818–1827.

Rubinstein, E., Charrin, S., and Tomlinson, M.G. (2013). Organisation of the tetraspanin web. In Tetraspanins, F. Berditchevski and E. Rubinstein, eds. (Springer), pp. 47–90.

Smith, M.E., and Ford, W.L. (1983). The recirculating lymphocyte pool of the rat: a systematic description of the migratory behaviour of recirculating lymphocytes. Immunology *49*, 83–94.

Springer, T.A. (1994). Traffic signals of lymphocyte recirculation and leukocyte emigration: the multistep paradigm. Cell *76*, 301–314.

Steeber, D.A., Green, N.E., Sato, S., and Tedder, T.F. (1996). Humoral immune responses in L-selectin-deficient mice. J. Immunol. *157*, 4899–4907.

Streeter, P.R., Berg, E.L., Rouse, B.T., Bargatze, R.F., and Butcher, E.C. (1988). A tissue-specific endothelial cell molecule involved in lymphocyte homing. Nature *331*, 41–46.

Tomlinson, M.G., Hanke, T., Hughes, D.A., Barclay, A.N., Scholl, E., Hunig, T., and Wright, M.D. (1995). Characterization of mouse CD53: epitope mapping, cellular distribution and induction by T cell receptor engagement during repertoire selection. Eur. J. Immunol. *25*, 2201–2205.

van Spriel, A.B., de Keijzer, S., van der Schaaf, A., Gartlan, K.H., Sofi, M., Light, A., Linssen, P.C., Boezeman, J.B., Zuidscherwoude, M., Reinieren-Beeren, I., et al. (2012). The tetraspanin CD37 orchestrates the alpha(4)beta(1) integrin-Akt signaling axis and supports long-lived plasma cell survival. Sci. Signal. *5*, ra82.

van Zelm, M.C., Smet, J., Adams, B., Mascart, F., Schandene, L., Janssen, F., Ferster, A., Kuo, C.C., Levy, S., van Dongen, J.J., et al. (2010). CD81 gene defect in humans disrupts CD19 complex formation and leads to antibody deficiency. J. Clin. Invest. *120*, 1265–1274.

Vinuesa, C.G., and Chang, P.P. (2013). Innate B cell helpers reveal novel types of antibody responses. Nat. Immunol. *14*, 119–126.

von Andrian, U.H., and Mackay, C.R. (2000). T-cell function and migration. Two sides of the same coin. N. Engl. J. Med. *343*, 1020–1034.

Walcheck, B., Alexander, S.R., St Hill, C.A., and Matala, E. (2003). ADAM-17-independent shedding of L-selectin. J. Leukoc. Biol. *74*, 389–394.

Wang, Y., Zhang, A.C., Ni, Z., Herrera, A., and Walcheck, B. (2010). ADAM17 activity and other mechanisms of soluble L-selectin production during death receptor-induced leukocyte apoptosis. J. Immunol. *184*, 4447–4454.

Wee, J.L., Schulze, K.E., Jones, E.L., Yeung, L., Cheng, Q., Pereira, C.F., Costin, A., Ramm, G., van Spriel, A.B., Hickey, M.J., et al. (2015). Tetraspanin CD37 regulates beta2 integrin-mediated adhesion and migration in neutrophils. J. Immunol. *195*, 5770–5779.

Xu, Y., Huang, Y., Cai, D., Liu, J., and Cao, X. (2015). Analysis of differences in the molecular mechanism of rheumatoid arthritis and osteoarthritis based on integration of gene expression profiles. Immunol. Lett. *168*, 246–253.

Yeung, L., Hickey, M.J., and Wright, M.D. (2018). The many and varied roles of tetraspanins in immune cell recruitment and migration. Front Immunol. *9*, 1644.

Yunta, M., and Lazo, P.A. (2003). Apoptosis protection and survival signal by the CD53 tetraspanin antigen. Oncogene *22*, 1219–1224.

Zuidscherwoude, M., Dunlock, V.E., van den Bogaart, G., van Deventer, S.J., van der Schaaf, A., van Oostrum, J., Goedhart, J., In 't Hout, J., Hammerling, G.J., Tanaka, S., et al. (2017). Tetraspanin microdomains control localized protein kinase C signaling in B cells. Sci. Signal. *10*, https://doi.org/10.1126/scisignal.aag2755.

iScience, Volume *23*

Supplemental Information

Tetraspanin CD53 Promotes Lymphocyte Recirculation by Stabilizing L-Selectin Surface Expression

Maria C. Demaria, Louisa Yeung, Rens Peeters, Janet L. Wee, Masa Mihaljcic, Eleanor L. Jones, Zeyad Nasa, Frank Alderuccio, Pamela Hall, Brodie C. Smith, Katrina J. Binger, Gunther Hammerling, Hang Fai Kwok, Andrew Newman, Ann Ager, Annemiek van Spriel, Michael J. Hickey, and Mark D. Wright

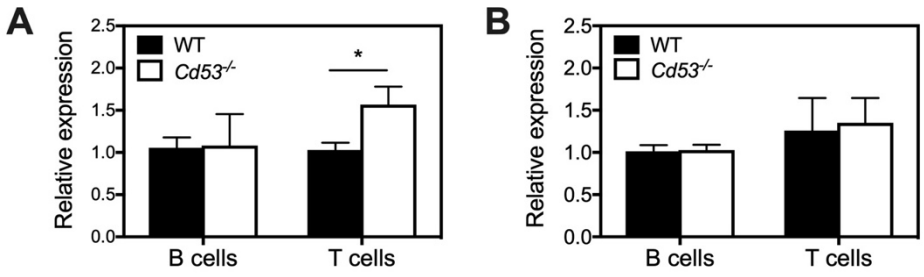

Figure S1. CD53 ablation does not decrease L-selectin mRNA expression, Related to Figure 3. Relative L-selectin mRNA expression in resting (A) and activated (B) WT and *Cd53*$^{-/-}$ T and B cells. Data are represented as mean + SEM, 6 mice per group pooled from 2-3 independent experiments, * $p \leq 0.05$, Student's two tailed t-test.

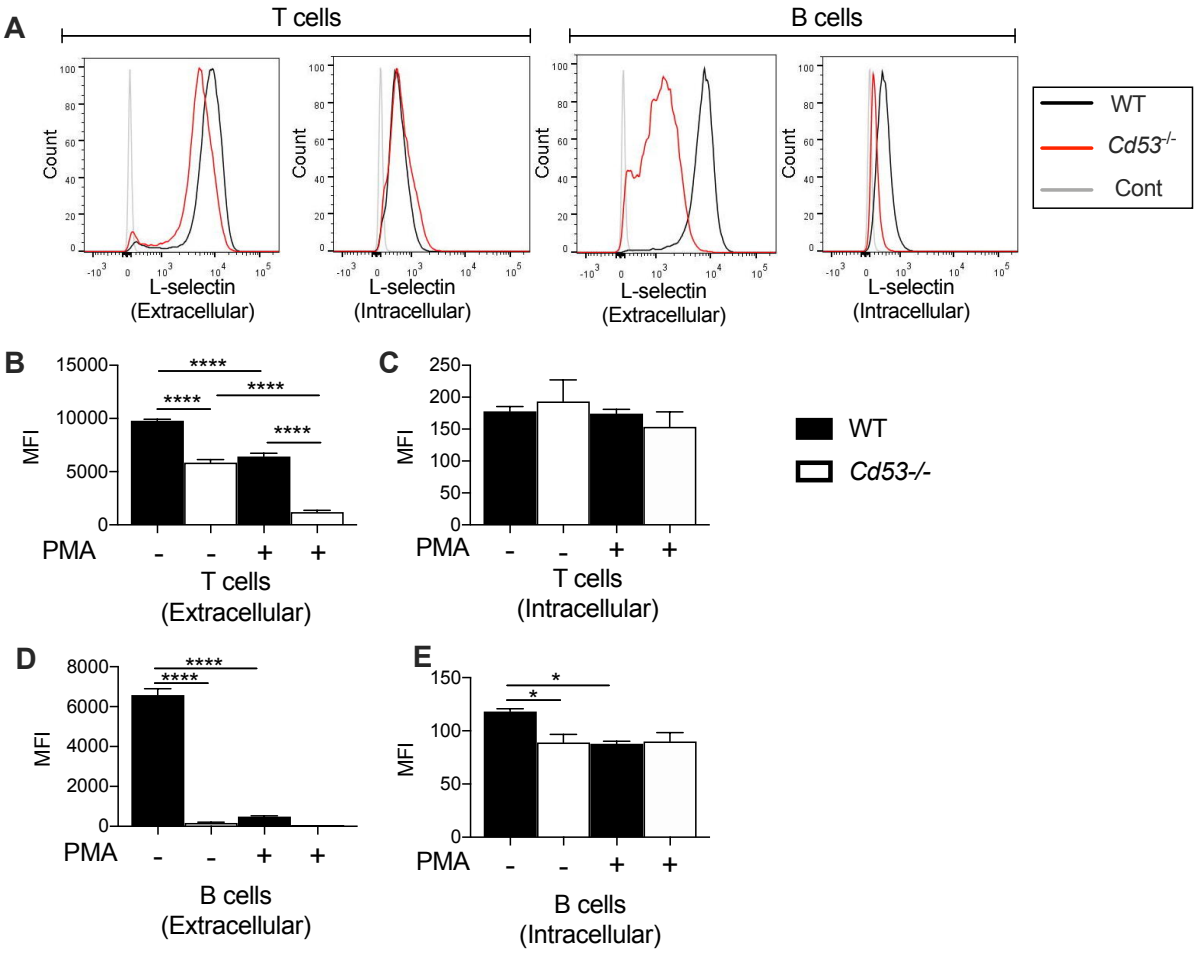

Figure S2. CD53 ablation does not lead to an accumulation of intracellular L-selectin, Related to Figure 3. (A) Representative flow cytometry histograms depicting intracellular and surface L-selectin expression in WT and *Cd53*$^{-/-}$ T and B cells. Quantification (mean fluorescent intensity, MFI) of surface (B and D) and intracellular (C and E) L-selectin expression in WT and *Cd53*$^{-/-}$ T cells (B and C) and B cells (D and E), as determined by flow cytometry with and without stimulation by PMA (5 minutes). Data are represented as mean + SEM, 5 mice per group, * $p \leq 0.05$, **** $p \leq 0.0001$, one-way ANOVA.

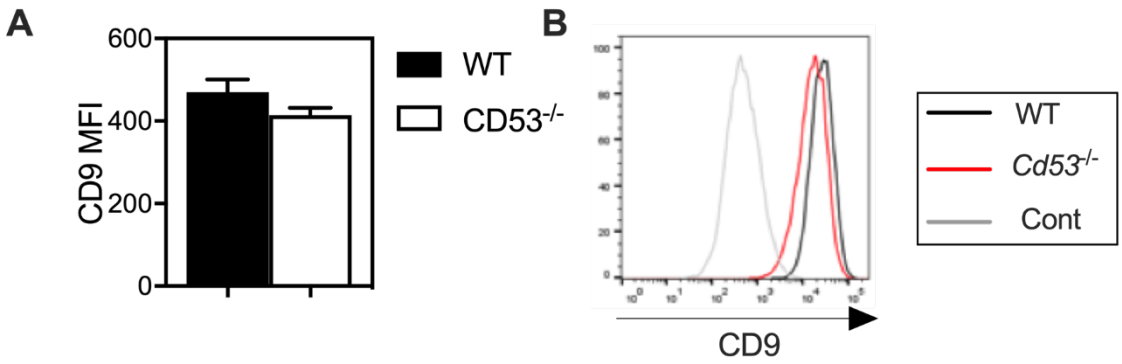

Figure S3. CD53 ablation has minimal effect on CD9 membrane expression, Related to Figure 3. (A) Quantification (mean fluorescent intensity, MFI) of CD9 expression on WT and *Cd53*$^{-/-}$ mouse T cells as determined by flow cytometry. Data are represented as mean + SEM, 3 mice per group. (B) Representative flow cytometry histograms illustrating human CD9 expression on WT and *hCd53*$^{-/-}$ human BJAB cells.

Transparent Methods

Mice

The generation of *Cd53*$^{-/-}$ mice has been recently described (Zuidscherwoude et al., 2017). Both *Cd53*$^{-/-}$ and C57BL/6J (wild-type, WT) mice were bred at the Monash Animal Research Platform (MARP), or Animal Research Laboratories (ARL) at Monash University (Clayton campus, Australia) or the Precinct Animal Centre (PAC) at the Alfred Research Alliance (formerly the Alfred Medical and Research Education Precinct (AMREP)) Melbourne, under specific-pathogen free conditions. All mice used for experimentation were between 4-12 weeks of age (or as indicated in text) and C57BL/6J age- and sex-matched mice were used as controls. The AMREP AS Animal Ethics Committee approved all experiments.

Lymphoid organ single cell suspensions

Lymphoid organs (including spleen, thymus, peripheral (inguinal and brachial) and mesenteric lymph nodes) were aseptically removed from WT and *Cd53*$^{-/-}$ mice. Blood (500 μL, collected by cardiac puncture) was placed into an equal volume of Alsever's solution to prevent coagulation. Single cell suspensions were prepared by disruption of organs in appropriate buffer. Bone marrow was flushed from the femur and tibia of WT and *Cd53*$^{-/-}$ mice using 25G needles. Erythrocytes in spleens, bone marrow and blood were lysed in ice-cold ACK lysis buffer. All suspensions were filtered through 70 μm strainers to remove cellular debris and washed. Viable cells were enumerated on a haemocytometer using trypan blue exclusion.

Flow cytometry

Cells were labelled with antibodies against a range of surface markers conjugated to a range of fluorochromes as follows: anti-B220 FITC* or APC Cy7 (RA3-6B2), anti-CD3 FITC or Cy5* (KT31.1), anti-CD4 Pacific Blue (RM4-5), anti-CD8 PE or APC Cy7 (53-6.7), anti-CD19 PE or eFluor450 (1D3), anti-CD53* (OX-79) and anti-L-selectin PE or PE Cy7 (MEL-14). Antibodies with an asterisk were purified and conjugated in house, all others were purchased from BD Pharmingen (San Diego, CA) or eBioscience (CA, USA). Antibodies were diluted to the appropriate titrated concentration in appropriate buffer, and cells stained on ice for 30 min. Cells were washed and resuspended in buffer containing 0.2% v/v propidium iodide prior to acquisition on a BD FACSCalibur, LSR II or LSRFortessa (BD Biosciences). Cells were analysed using FlowJo Software (TreeStar Inc., OR, USA) following exclusion of doublets and propidium iodide-positive cells. For assessment of surface and intracellular L-selectin, non-permeabilised lymph node cells were first stained for surface L-selectin using PE-conjugated

anti-L-selectin (clone MEL-14) at a concentration (8 μg /ml) determined in pilot experiments to minimize any further staining achieved by subsequent exposure to anti-L-selectin-FITC (data not shown). Cells were subsequently washed, fixed/permeabilized (BD Cytofix/Cytoperm, BD Biosciences Pharmingen) and stained for intracellular L-selectin using FITC-conjugated anti-L-selectin (5 μg/ml). Surface and intracellular L-selectin levels were determined via flow cytometric analysis, identifying T cells as TCR beta chain$^+$ cells (clone H57-597, conjugated to APC), and B cells as CD19$^+$ cells (clone 1D3, conjugated to BV711).

B and T cell isolation

B cells were isolated by negative selection from the spleens of WT and *Cd53*$^{-/-}$ mice using the Dynabeads Mouse CD43 (Untouched B cells) kit (Life Technologies, CA, USA) according to the manufacturer's instructions. Negative selection by magnetic bead depletion was used for T cell isolation as previously described (Sheng et al., 2009).

Homing Assays

WT splenocyte homing assay. Single cell suspensions of WT spleens were prepared as described above. Splenocytes were labeled with 0.5 μM CFSE (10 mins, 37°C; Life Technologies, CA, USA). 3x10^7 splenocytes in 100 μL PBS were injected i.v. into WT and *Cd53*$^{-/-}$ mice. Spleens, peripheral (inguinal and brachial) LNs, mesenteric LNs and blood were harvested 48 h later and single cell suspensions analysed by flow cytometry for the presence of CFSE$^+$ splenocytes, including CFSE$^+$ CD19$^+$ B cells and CFSE$^+$ CD3$^+$ T cells. Absolute CFSE$^+$ cell number in each organ was calculated based on frequencies of CFSE$^+$ cells and organ cell counts.

B and T cell homing assays. B and T cells from WT and *Cd53*$^{-/-}$ mice were isolated and labelled with CFSE as above. WT cells were also labelled with 1 μM Cell Proliferation Dye eFluor670 (referred to in this article as Cell Tracker 670; 10 min, 37°C; eBioscience, CA, USA) for use as an internal control. 10^7 WT or *Cd53*$^{-/-}$ CFSE-labelled B or T cells were mixed in equal numbers with Cell Tracker 670-labelled WT B or T cells and injected i.v. into WT mice in 100 μL PBS. The injected cell mixture was analysed by flow cytometry to determine the ratio of fluorescently-labelled cells in the starting preparation. Lymphoid organs were harvested after 48 h and analysed by flow cytometry for fluorescently-labelled CD3$^+$ T cells or CD19$^+$ B cells. Homing indices were calculated according to the following formula:

Homing index = (Sample:Internal control)$_{organ}$ / (Sample:Internal control)$_{injected}$ (Arbones et al., 1994).

Gene expression by real-time quantitative PCR (qPCR)

Purified B and T cells were activated for 18 h with 10 μg/mL of LPS (from E. coli K12; InvivoGen, CA, USA) or 10 μg/mL immobilised anti-CD3 plus 1 μg/mL soluble anti-CD28, respectively. Activated cells were analysed by flow cytometry for the upregulation of CD69 and/or CD25. RNA was isolated from purified B and T cells (naïve or activated) using the spin purification protocol from the SV Total RNA Isolation System (Promega, WI, USA) and converted to cDNA through the use of an RNA to cDNA kit according to manufacturer instructions (Life Technologies, CA, USA). Levels of mouse L-selectin and 18S mRNA were measured using predesigned Taqman® Gene Expression Assays (Catalog Mm_0041291_m1 and Mm_03928990_g1; Life Technologies, CA, USA). qPCR was performed according to manufacturer instructions in an ABI Prism® 7900HT Sequence Detection System (Life Technologies).

L-selectin shedding assays

2-2.5x10^6 cells/well of purified wild-type and *Cd53*$^{-/-}$ mouse T lymphocytes were activated at 37°C with 50 ng/mL (80 nM) PMA in 0.5% BSA/RPMI at designated time points (2.5, 5, 15, and 30 min) to induce L-selectin shedding from the cell surface. When required, cells were pre-incubated at 37°C with inhibitors for 10 min prior to the addition of PMA. A broad spectrum metalloprotease inhibitor GM6001 (Tocris Bioscience, Bristol, UK), TAPI-1 (an inhibitor of ADAM17, Tocris Bioscience), ADAM17-specific inhibitory antibody A9(B8) (Kwok et al., 2014), and GI254023X (a potent inhibitor of ADAM10, Tocris Bioscience) were added at final concentrations of 100 μM, 20 μM, 200 nM or 5 μM respectively. An unstimulated control (no PMA) was included, where 0.5% BSA/RPMI was added to cells instead. All reactions were stopped by placing wells on ice. Cells were then centrifuged at 1,800 rpm for 5 min at 4°C. The supernatant was harvested for ELISA experiments, and cells were resuspended in FACS buffer. 5x10^5 cells were stained with anti-CD3 FITC, and anti-L-selectin PE. Levels of L-selectin surface expression were determined by flow cytometry on the FACSCalibur (BD Biosciences) or the LSRFortessa (BD Biosciences). A sandwich ELISA was used to determine soluble L-selectin levels in supernatants from activated T and B cells. Wells were coated with anti-mouse L-selectin (clone 95226; R&D Systems, MN, USA) and L-selectin detected by

biotinylated anti-mouse L-selectin (clone 95218; R&D Systems, MN, USA). Recombinant mouse L-selectin/CD62L Fc Chimera was used as a standard in all assays (R&D Systems, MN, USA). Streptavidin-HRP, TMB (Life Technologies, CA, USA) and 1M HCl were used for detection. OD was determined at 450 nm (Multiskan Go plate reader, ThermoFisher Scientific). For long-term assays to measure spontaneous L-selectin shedding without PMA activation, $2x10^6$ cells were incubated as above and for 1, 2 or 3 h. Cells were harvested and stained with antibodies to L-selectin, CD3 or B220 as required, prior to acquisition on a flow cytometer.

Analysis of human *Cd53*$^{-/-}$ B cells

Monoclonal and polyclonal *Cd53*-deficient human BJAB cells were generated by CRISPR-Cas9 technology as previously described (Zuidscherwoude et al., 2017). DNA electroporation of WT and CD53-deficient cells was performed with the Neon® Transfection System MPK5000 (Thermo Fisher Scientific, MA, USA). Per transfection, 4.8×10^6 cells were washed in PBS and resuspended in 120 µL resuspension buffer R and mixed with 0.5 µg pmaxGFP™ (Cell Line Optimization Solution Box; Lonza, Basel, CH) and 1.5 µg L-selectin DNA. A volume of 100 µL was transferred to a Neon® Electroporation Tube in a 100 µL Neon® Tip (Neon® Transfection System 100 µL Kit; MPK10096, Invitrogen). A single electroporation pulse of 1350V for 40 ms was given. After transfection, cell suspensions were resuspended in 3 mL RPMI without antibiotics and cultured overnight at 37°C and 5% CO_2.

Transfected cells were kept at optimal densities for 48 h. Three groups of 2×10^5 cells per transfected and untransfected controls were washed in PBS and resuspended in either PBA (1x PBS, 1% BSA, 0.05% NaN_3), 1µg/mL mouse IgG1 isotype (clone MOPC-21; BioLegend, SD, USA) or 1 µg/mL mouse anti-human anti-L-selectin (clone DREG56; Novus, Manchester, UK) and incubated on ice for 30 min. Cells were washed in PBS and resuspended in either PBA (PBS), or goat anti-mouse IgG1 Alexa Fluor® 647 (Invitrogen, MA, USA) and incubated in the dark on ice for 30 min. Cells were then washed in PBS and resuspended in 150 µL PBA and analyzed on MACSQuant® Analyzer 10 flow cytometer (Milteny Biotec, Bergisch Gladbach, DE).

Induction and measurement of immune responses

Mice were immunised intraperitoneally (i.p.) or intradermally (i.d.) at the base of the tail with

100 μg $NP_{(25-28)}$-KLH (Biosearch Technologies, Novato, CA) precipitated in alum (10% w/v) as an adjuvant (T-cell dependent responses) or with 50 μg $NP_{(0.6)}$-LPS or $NP_{(40)}$-AECM-FICOLL in PBS (Biosearch Technologies, Novato, CA) (T-cell independent responses). A pre-bleed (submandibular) was taken before immunisation and submandibular bleeds were taken weekly from immunised mice. ELISAs to determine isotype specific antibody responses against NP were performed as previously described (van Spriel et al., 2009).

EAE was induced by MOG_{35-55} immunisation following a standard protocol (Chan et al., 1997). Briefly, mice were immunised subcutaneously in each flank with 100 μg MOG_{35-55} (GL Biochem, Shanghai, China) emulsified in CFA supplemented with 4 mg/mL of *Mycobacterium tuberculosis* H37Ra (DICO laboratories, USA) and also injected on the same day i.p. with 350 ng/mouse Pertussis toxin (List Biological laboratories, USA) in PBS. Forty-eight hours later mice were re-injected with 350 ng/mouse Pertussis toxin i.p. Mice were monitored daily for weight loss and clinical signs of EAE. Clinical scores were assigned according to the following: 0, no disease; 1, tail weakness; 2, tail paralysis and hind limb weakness; 3, hind limb paralysis; 4, hind and forelimb paralysis; 5 death. For ethical reasons mice were culled when a clinical score of 3 was reached.

Statistical analysis

The student's two tailed t-test, or Mann-Whitney test, or 2-way ANOVA (for EAE) was used to for statistical comparisons between data sets. GraphPad Prism 6 software (CA, USA) was used for statistical analysis.

Supplemental References

Arbones, M.L., Ord, D.C., Ley, K., Ratech, H., Maynard-Curry, C., Otten, G., Capon, D.J., and Tedder, T.F. (1994). Lymphocyte homing and leukocyte rolling and migration are impaired in L-selectin-deficient mice. Immunity *1*, 247-260.

Chan, V.W., Meng, F., Soriano, P., DeFranco, A.L., and Lowell, C.A. (1997). Characterization of the B lymphocyte populations in Lyn-deficient mice and the role of Lyn in signal initiation and down-regulation. Immunity *7*, 69-81.

Kwok, H.F., Botkjaer, K.A., Tape, C.J., Huang, Y., McCafferty, J., and Murphy, G. (2014). Development of a 'mouse and human cross-reactive' affinity-matured exosite inhibitory human antibody specific to TACE (ADAM17) for cancer immunotherapy. Protein Eng Des Sel *27*, 179-190.

Sheng, K.C., van Spriel, A.B., Gartlan, K.H., Sofi, M., Apostolopoulos, V., Ashman, L., and Wright, M.D. (2009). Tetraspanins CD37 and CD151 differentially regulate Ag presentation and T-cell co-stimulation by DC. Eur J Immunol *39*, 50-55.

van Spriel, A.B., Sofi, M., Gartlan, K.H., van der Schaaf, A., Verschueren, I., Torensma, R., Raymakers, R.A., Loveland, B.E., Netea, M.G., Adema, G.J.*, et al.* (2009). The tetraspanin protein CD37 regulates IgA responses and anti-fungal immunity. PLoS Pathog *5*, e1000338.

Zuidscherwoude, M., Dunlock, V.E., van den Bogaart, G., van Deventer, S.J., van der Schaaf, A., van Oostrum, J., Goedhart, J., In 't Hout, J., Hammerling, G.J., Tanaka, S.*, et al.* (2017). Tetraspanin microdomains control localized protein kinase C signaling in B cells. Science signaling *10*.